Carbohydrate Polymers 78 (2009) 422–431

Contents lists available at ScienceDirect

Carbohydrate Polymers

journal homepage: www.elsevier.com/locate/carbpol

Cassava bagasse cellulose nanofibrils reinforced thermoplastic cassava starch

Eliangela de M. Teixeira [a], Daniel Pasquini [b], Antônio A.S. Curvelo [a], Elisângela Corradini [c], Mohamed N. Belgacem [d], Alain Dufresne [d,*]

[a] Instituto de Química de São Carlos, Universidade de São Paulo, C.P. 780, 13560-970 São Carlos, SP, Brazil
[b] CICECO e Departamento de Química, Universidade de Aveiro, 3810-193 Aveiro, Portugal
[c] Departamento de Engenharia de Materiais, Universidade Federal de São Carlos, C.P. 676, 13560-095 São Carlos, SP, Brazil
[d] Grenoble Institute of Technology, The International School of Paper, Print Media and Biomaterials (Grenoble INP – Pagora), BP65, 38402 Saint Martin d'Hères Cedex, France

ARTICLE INFO

Article history:
Received 25 February 2009
Received in revised form 5 April 2009
Accepted 27 April 2009
Available online 12 May 2009

Keywords:
Cassava bagasse
Thermoplastic starch
Cellulose nanofibrils
Nanocomposites

ABSTRACT

Cellulose cassava bagasse nanofibrils (CBN) were directly extracted from a by-product of the cassava starch (CS) industry, viz. the cassava bagasse (CB). The morphological structure of the ensuing nanoparticles was investigated by scanning electron microscopy (SEM), transmission electron microscopy (TEM), atomic force microscopy (AFM), presence of other components such as sugars by high performance liquid chromatography (HPLC), thermogravimetric analysis (TGA), and X-ray diffraction (XRD) experiments. The resulting nanofibrils display a relatively low crystallinity and were found to be around 2–11 nm thick and 360–1700 nm long. These nanofibrils were used as reinforcing nanoparticles in a thermoplastic cassava starch matrix plasticized using either glycerol or a mixture of glycerol/sorbitol (1:1) as plasticizer. Nanocomposite films were prepared by a melting process. The reinforcing effect of the filler evaluated by dynamical mechanical tests (DMA) and tensile tests was found to depend on the nature of the plasticizer employed. Thus, for the glycerol-plasticized matrix-based composites, it was limited especially due to additional plasticization by sugars originating from starch hydrolysis during the acid extraction. This effect was evidenced by the reduction of glass vitreous temperature of starch after the incorporation of nanofibrils in TPSG and by the increase of elongation at break in tensile test. On the other hand, for glycerol/sorbitol plasticized nanocomposites the transcrystallization of amylopectin in nanofibrils surface hindered good performances of CBN as reinforcing agent for thermoplastic cassava starch. The incorporation of cassava bagasse cellulose nanofibrils in the thermoplastic starch matrices has resulted in a decrease of its hydrophilic character especially for glycerol plasticized sample.

1. Introduction

Starch is a widely available, renewable, low cost, and biodegradable agro-polymer. For these reasons starch generates a great interest and it is considered as a promising alternative to synthetic polymers for packaging applications. The general procedure to process starchy materials involves the granular disruption by the combination of temperature, shear, and a plasticizer, which is usually water and/or glycerol (Averous, 2004). The resultant material is known as thermoplastic starch (TPS). However, the use of TPS is limited in industrial applications, owing to its low resistance to mechanical stresses and humidity (Anglès & Dufresne, 2000; Averous, 2004; Curvelo, de Carvalho, & Agnelli, 2001). Several strategies have been investigated to minimize or even overcome these poor characteristics. These strategies involve (i) the chemical modification of starch (esterification and cross-linking) (Averous, 2004; Nabeshima & Grossmann, 2001), (ii) blending with other polymers such as poly (vinyl alcohol) and biodegradable polyesters such as poly (ε-caprolactone), polyhydroxyalkanoate, polyesteramide, and poly(butylene succinate adipate) (Averous, 2004), and (iii) the use of different types of fibers or microfibrils in association with TPS (Averous, 2004; Curvelo et al., 2001; Dufresne, Dupeyre, & Vignon, 2000; Wolledorfer & Bader, 1998).

Cellulose nanoparticles have been synthesized in spherical form (Pu et al., 2007; Zhang, Elder, Pu, & Ragauska, 2007; Zhang, Jiang, Dang, Elder, & Ragauska, 2008), rod-like highly crystalline nanocrystals (Azizi Samir, Alloin, & Dufresne, 2005; Dufresne, 2006, 2008; Lima & Borsali, 2004) which are obtained by acid hydrolysis of cellulosic fibers, and microfibrillated cellulose (MFC) resulting from disintegration of cellulose fibers under high shearing and impact forces. For the latter, a network of interconnected microfibrils with dimensions of 10–100 nm thick and several microns long are obtained (Cherian et al., 2008; Pääkko et al., 2007; Gardner, Oporto, Mills, & Samir, 2008). The degree of crystallinity of MFC or cellulose microfibrils is usually low since the amorphous domains of cellulose remain intact (Pääkko et al., 2007).

Cellulose nanocrystals or whiskers have been used to reinforce starchy material (Anglès & Dufresne, 2000, 2001; Kvien, Sugiyama, Votrubec, & Oksman, 2007; Mathew & Dufresne, 2002). However,

* Corresponding author. Tel.: +33 476 82 69 95; fax: +33 476 82 69 33.
E-mail address: Alain.Dufresne@efpg.inpg.fr (A. Dufresne).

0144-8617/$ - see front matter © 2009 Elsevier Ltd. All rights reserved.
doi:10.1016/j.carbpol.2009.04.034

in these previous studies, the nanocomposite films were obtained by the casting method instead of conventional melt processing techniques commonly used for synthetic polymers. Cellulose whiskers reinforced starch nanocomposite materials are largely complex systems because of the presence of four components (starch, cellulose, main plasticizer, and water) and competitive interactions are likely to occur between these constituents. An example of this complexity is the transcrystallization phenomenon of amylopectin chains observed on the surface of cellulose whiskers due to the accumulation of the plasticizers (glycerol and water) in the vicinity of the cellulose/amylopectin interfacial zone (Anglès & Dufresne, 2000). This phenomenon was reported to interfere with inter whiskers hydrogen-bonding forces and to hinder the stress transfer at the filler/matrix interface, resulting in poor mechanical properties of the ensuing nanocomposites (Anglès & Dufresne, 2000, 2001; Mathew & Dufresne, 2002).

Cassava (*Manihot esculenta*) is a root crop largely grown in tropical countries such as Brazil. It is a starch-rich material, also containing proteins, lipids, lignocellulosic fibers and sugars. The industrial exploitation of cassava starch (CS) involves the elimination of soluble sugars and the separation of fibers resulting in a purified starch and a solid residue called cassava bagasse (CB). The cassava bagasse is mainly composed of water (70–80 wt%), residual starch and cellulose fibers. The cellulose fibers content ranges between 15 and 50 wt% of the total solid residue (dry weight basis), the remainder being residual starch (Matsui et al., 2004; Teixeira, Da Róz, de Carvalho, & Curvelo, 2005). This material is destined to animal feed and has potential application for the production of lactic acid by bacterias (John, Gangadharan, & Nampoothiri, 2008; John, Sukumaran, Nampoothiri, & Pandey, 2007; Ray, Mohapatra, Panda, & Kar, 2008), production of ethanol (Martín, Lopez, Plasencia, & Hernández, 2006; Martín & Thomsen, 2007; Ray et al., 2008), and removal of heavy metal íons (Cd(II), Cu(II), and Zn(II)) from wastewater (Ngah & Hanafiah, 2008). Therefore, this residue contains both a great deal of residual starch and a considerable quantity of natural fibers. These characteristics suggest the possibility of using the bagasse as a source of cellulose fibers for the extraction of new nanocellulose structures. Cellulose nanostructures from agricultural residues such as banana farming (Cherian et al., 2008; Zuluaga, Putaux, Restrepo, Mondragon, & Gañán, 2007; Zuluaga et al., 2009) and wheat straw and soy hulls (Alemdar & Sain, 2008) have already been reported.

In the present work, cellulose nanofibrils obtained from cassava bagasse fibers without any purification have been prepared and characterized by transmission electron microscopy (TEM), atomic force microscopy (AFM), X-ray diffraction (XRD), and thermogravimetric analysis (TGA). This nanocellulose has been incorporated in a thermoplastic cassava starch matrix to improve both the mechanical properties and the hydrophobic character of starch-based plastic. Two types of plasticizers, viz. glycerol and sorbitol, were investigated to process the nanocomposites. So, the main originality of the work is that both the matrix and the reinforcing phase are from natural origin and extracted from the same plant leading to all-cassava nanocomposite materials. The nanocomposites were obtained by a melting process using a torque rheometer. The morphology and properties of resulting materials were characterized by scanning electron microscopy (SEM), XRD, dynamic mechanical analysis (DMA), tensile testing, and water uptake.

2. Experimental

2.1. Materials

Cassava starch (CS) containing about 18% amylose and dried cassava bagasse (CB) containing about 17.5 wt% fibers and 82.5 wt% starch were kindly supplied by Corn Products Brazil. Reagent grade glycerol (Synth) and sorbitol (Acrós) were used as plasticizers. Sulfuric acid (Synth) and cellulose membrane (Sigma–Aldrich) was used for cellulose hydrolysis. Stearic acid (Oxiteno) was used as processing agent of nanocomposites.

2.2. Preparation of cassava bagasse cellulose nanofibers (CBN)

Cellulose nanofibers were extracted from cellulose fibers present in CB. About 10 g of CB were dispersed in 200 mL of 6.5 M sulfuric acid into a flask under mechanical stirring. Hydrolysis was performed at 60 °C under vigorous stirring for 40 min. The excess of sulfuric acid was removed from the ensuing suspension by centrifugation at 8000 rpm for 10 min. After that, the suspension was submitted to dialysis against distilled water using a cellulose membrane until the pH reached 6–7. The resulting suspension was submitted to an ultrasonic treatment for 5 min and stored in a refrigerator.

2.3. Preparation of nanocomposites reinforced with CBN

When using sorbitol as the unique plasticizer, it was found that the resulting material was brittle and difficult to manipulate after processing. Then, not only glycerol but also a mixture of glycerol and sorbitol (1:1) rather than pure sorbitol was used. For the preparation of nanocomposites, the CS was first mixed with glycerol or a glycerol/sorbitol mixture (30 wt%, based on dry material) in polyethylene bags until a homogeneous material was obtained. Stearic acid (0.5 wt%) was added to each mixture. Nanocomposite materials with different weight fractions of CBN (0, 5, 10, and 20 wt% of CBN, dry starch basis) were prepared by addition of the appropriated amount of aqueous suspension. Previously to the addition of the suspension in the starch/glycerol or starch/glycerol/sorbitol matrix, the suspension was submitted again to an ultrasonic treatment for 5 min. The final water content was adjusted to 20 wt% (water + suspension, dry starch basis) for all samples. The composition and codification of the samples are collected in Table 1. The previous mixtures were processed at 140 ± 10 °C in a Haake Rheomix 600 batch mixer equipped with roller rotors rotating at 60 rpm. The mixing time was fixed at 6 min. The processed samples were then hot-pressed at 140 °C into 1 and 2 mm thick plates. This temperature is supposed to be low enough to avoid any glycerol volatilization (the boiling point of glycerol is 290 °C) and thermal degradation of CBN.

2.4. Microscopic analyses

2.4.1. Scanning electron microscopy (SEM)

The morphology of CB, CBN (the suspension was dried at 50 °C, coated with a thin gold film) and fractured surface (under liquid

Table 1
Codification and composition of CBN reinforced thermoplastic cassava starch nanocomposites.

Sample	CS (wt%)	Glycerol (wt%)	Sorbitol (wt%)	Water (wt%)	CBN (wt%)
TPSG	50	30	0	20	0
TPSG5	50	30	0	15	5
TPSG10	50	30	0	10	10
TPSG20	50	30	0	0	20
TPSGS	50	15	15	20	0
TPSGS5	50	15	15	15	5
TPSGS10	50	15	15	10	10
TPSGS20	50	15	15	0	20

CS, cassava bagasse; CBN, cassava bagasse nanofibers; for all compositions 0.5% stearic acid was added.

nitrogen) of the nanocomposite plates were investigated by scanning electron microscopy (SEM) using a Leo Scanning Electron Microscope (LEO-400) instrument.

2.4.2. Transmission electron microscopy (TEM)

An aliquot of CBN suspension was diluted and sonified for 5 min (Branson 450 sonifier). A drop of this resultant diluted suspension was deposited on a carbon microgrid net (400 meshes) and the grid was stained with a 1.5% solution of uranyl acetate and dried at room temperature. Transmission electron micrographs (TEM) images were obtained using a Philips CM200 transmission electron microscope with an acceleration voltage of 80 kV.

2.4.3. Atomic force microscopy (AFM)

The AFM measurements were performed with a Dimension V (Veeco) atomic force microscope. All images were obtained in tapping mode with scan rate of 1 Hz and using Si tips with curvature radius of 14 nm and angle of sloping tip wall of about 12° (nominal values), attached to a cantilever (V-shape) of spring constant of 42 N m^{-1}. A drop of diluted nanofibers aqueous suspension (sonicated) was allowed to dry on optical glass substrate at room temperature and analyzed subsequently.

2.5. High performance liquid chromatography (HPLC) from nanofibers suspension

The possible presence of sugars in the CBN suspension was investigated using HPLC. The solution of CBN was filtered in a SEP PAK C18 membrane (0.45 μm, Waters) and analyzed using a SHIMADZU, model CR 7A with detector IR SHIMADZU R10-6A and a column Aminex HPX 87H (300 mm × 7.8 mm, BIORAD). The eluent (flow rate of 0.6 mL min^{-1}) was H_2SO_4, 0.005 mol L^{-1} solution. Two mixtures of various combinations sugars (Synth and Merck) and acetic and formic acid (0.0032 g mL^{-1} of each component) were used as standard. These were coded as

Standard 1: glucose, maltose, fructose, and sucrose
Standard 2: cellobiose, glucose, xylose, arabinose, formic acid, and acetic acid.

This determination was only qualitative because part of the sugars was probably removed after successive centrifugations and during the dialysis. In addition, because of the high viscosity of the suspension the filtration process for HPLC analysis may not be as effective. An aliquot of 20 μL of CBN suspension was analyzed after fivefolds dilution in water.

2.6. X-ray diffraction (XRD)

The X-ray diffraction patterns were measured for both CB and dried CBN suspension with an X-ray diffractometer using Cu Kα radiation at 40 kV and 30 mA. Scattered radiation was detected in the range 2θ = 5–40°, at a speed of 2°/min. The crystallinity (I_c) was estimated by means of Eq. (1) using the height of the 200 peak (I_{200}, 2θ = 22.6°) and the minimum between the 200 and 110 peaks (I_{am}, 2θ = 18°). I_{200} represents both crystalline and amorphous material while I_{am} represents amorphous material.

$$I_c = (I_{200} - I_{am}/I_{200}) \times 100 \quad (1)$$

The diffractograms for nanocomposites were recorded after conditioning the samples (10 days) in a 53% relative humidity (RH) atmosphere at 25 ± 2 °C. Their crystallinity index was estimated by the height ratio of the diffraction peak (B-type at 2θ = 16.8° and V_H-type at 2θ = 19.6°) and the baseline of the diffractogram, as proposed by Hulleman, Kalisvaart, Janssen, Feil, and Vliegenthart (1999).

2.7. Thermogravimetric analysis

The thermogravimetric analysis (TGA) was performed with a Shimadzu model TGA-50TA for CS, CB, and CBN (suspension aliquot was dried in air-circulating oven at 50 °C). The sample (9.0 ± 1.0 mg) was heated from 25 to 900 °C under air atmosphere with a flow rate of 20 mL min^{-1} and using a platinum crucible. The heating rate was 20 °C min^{-1}.

2.8. Nanocomposite conditioning and water uptake

The nanocomposite samples were dried at 70 °C up to a constant weight. They were then conditioned prior to each analysis in hermetic containers at 25 ± 2 °C and in a 53% RH atmosphere in equilibrium with a saturated solution of $Mg(NO_3)_2{\cdot}6H_2O$, as stipulated in ASTM E 104. Water uptake experiments were conducted on circular specimens, 8 mm diameter, cut from the hot-pressed plates of nanocomposites, which were 2 mm thick. The water uptake at equilibrium was computed from the gain in weight.

2.9. Dynamic mechanical analysis (DMA)

Dynamical mechanical analysis were carried out with a Polymer Laboratories DMTA MK-II instrument, in accordance with ASTM D5023, using a three-point bending method. The dynamic storage modulus (E') and loss factor ($\tan\delta$) were measured as a function of temperature from −100 to 100 °C, at a constant heating rate of 2 °C min^{-1} and displacement amplitude of 64 μm, at a frequency of 1 Hz. The main relaxation temperature (T_α), associated to the glass transition temperature of the samples, was determined as the temperature at the maximum of the $\tan\delta$ peak displayed in the $\tan\delta$ versus temperature curves.

2.10. Tensile tests

The tensile tests were performed with an Instron 5569 Universal Test instrument equipped with a load cell of 200 kgf. The samples, previously conditioned at 53% relative humidity between 24 and 25 °C for 10 days, were tested in accordance with the ASTM D638M-96 type II requirements, using a crosshead speed of 50 mm min^{-1}. The tensile modulus was calculated by the instrument software using the slope of the initial portion of the stress–strain curves. The mechanical tensile data were averaged over at least five specimens.

3. Results and discussion

3.1. Morphological and structural characterization of CBN

Fig. 1 shows a SEM micrograph of (a) CB and of (b) dried CBN. For CB, granular and partially disrupted starch can be observed besides cellulose fibers. After acid hydrolysis of CB a continuous and paper-like fibrous network film was observed. This dense web-like structure consists of cellulose nanofibrils. However, individual nanoparticles cannot be distinguished.

Fig. 2 shows the physical aspect of CBN suspension and the TEM micrographs of a dilute suspension of them. The clear spots arise from the uranyl acetate. The suspension contained cellulose fragments consisting of long and curved elongated nanoparticles. The fact that some of these rod-like nanoparticles are not perfectly straight could indicate that the hydrolysis of cellulose microfibrils was not complete. Their morphology looks like microfibrillated cellulose (Pääkko et al., 2007) with high length (micrometer scale) and low diameter (15–20 nm). It is worth noting that during the sonication step, the suspension behaved as a gel. This is obviously

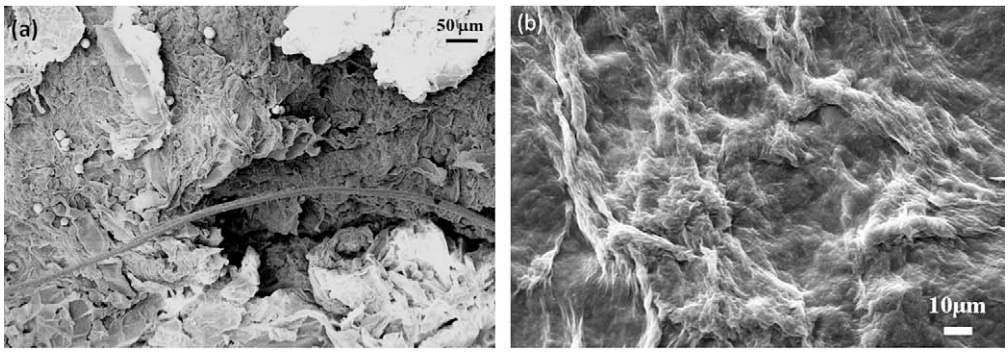

Fig. 1. Scanning electron micrograph of (a) CB and (b) dried CBN.

ascribed to the individualization of the nanoparticles but it could also suggest the presence of long and entangled nanoscale cellulose. The diameter and length of the CBN was found to be in the range of 2–11 and 360–1700 nm, respectively.

The AFM image (Fig. 3) also showed the existence of CBN as entangled nanoscale cellulose. The determination of the diameter of the nanoparticles gives a higher value (25 ± 7 nm) than the one determined from TEM observation. Kvien, Tanem, and Oksman (2005) concluded that AFM analysis overestimates the width of the nanocellulose due to the tip-broadening effect. The length of the nanoparticles could not be determined from AFM observation.

The total solid content of the suspension probably consists in a mixture of CBN, partially hydrolyzed starch and low molecular weight sugars. Indeed, the low molecular weight compounds were most probably not eliminated during the dialysis step because of the short dialysis time necessary to remove the acid used for the hydrolysis, i.e., until neutral pH was reached.

Fig. 4 shows the standard and CBN sample chromatogram of HPLC analysis and Table 2 the probable components of the suspension although nanocellulose. Thus, the presence of sugars (see Table 2) in the CBN suspension could be confirmed.

The final solid content in the suspension was about 27.5 ± 1.0 wt%. It will be referred as CBN even if this solid residue contains other components than nano cellulosic structures. The presence of these impurities in the suspension could explain the aspect of the CBN films observed by SEM (Fig. 1). The expected porosity of the film could be filled with these impurities.

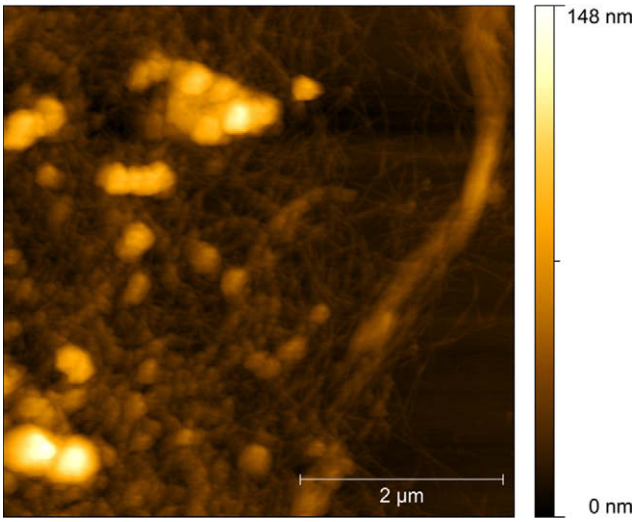

Fig. 3. AFM image of CBN.

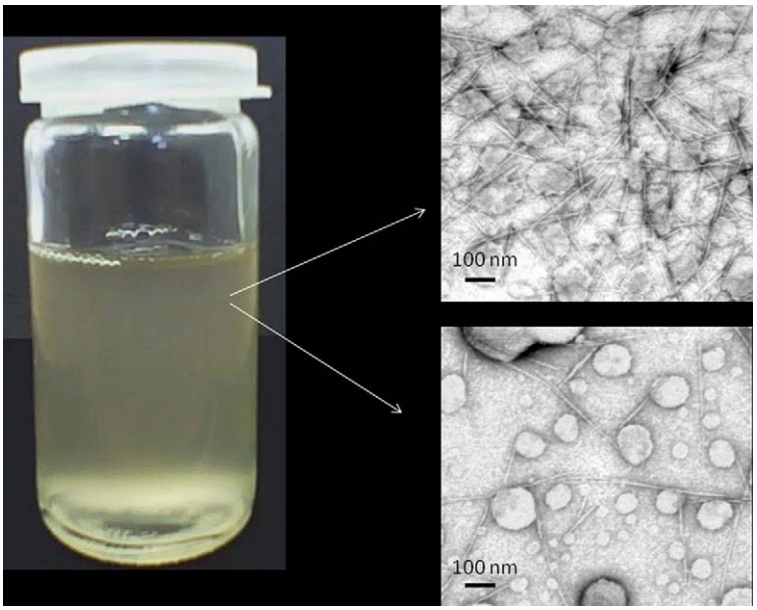

Fig. 2. Physical aspect and transmission electron micrographs from a dilute suspension of CBN.

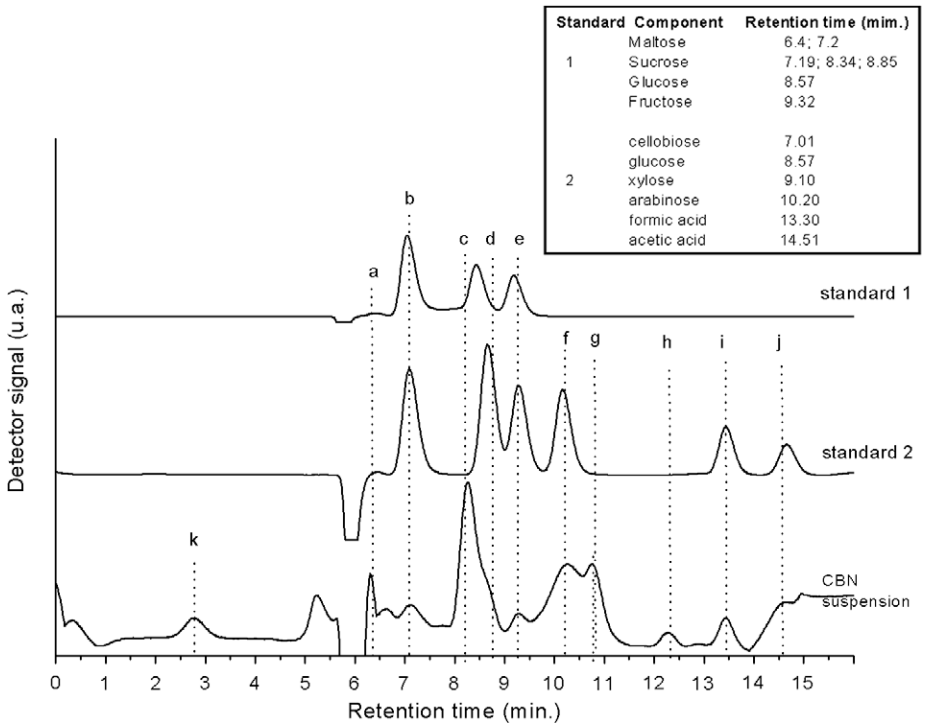

Fig. 4. The standards and CBN sample chromatogram of HPLC analysis. Probable components: a, maltose; b, maltose, cellobiose and/or sucrose; c, glucose and/or sucrose; d, sucrose; e, fructose and xylose; f, arabinose; g, n.i.(*); h, n.i.(*); i, formic acid; j, acetic acid, k, n.i.(*), not identified.

The X-ray diffraction patterns recorded for CB and CBN (obtained after water evaporation) are shown in Fig. 5. Both diffractograms display two well-defined peaks around $2\theta = 12.5^{o}$ and $2\theta = 22.5^{\circ}$ characteristic of cellulose (Klemm, Heublein, Fink, & Bohn, 2005). From Fig. 5 it can be observed that the acid treatment results in a narrowing and an increase of the magnitude of both peaks most probably because of the higher crystallinity level of the hydrolyzed cellulosic compared to the original fibers present in CB. The crystallinity index was calculated and found to be 43.7% and 54.1% for the CB and CBN, respectively. The apparent relatively low degree of crystallinity of the hydrolyzed residue confirms the presence of other compounds than nanocellulose and also suggests that amorphous cellulosic domains remain. It agrees with TEM observations and indicates that not really nanocrystals but rather partially hydrolyzed fibrillated cellulose with nanoscale diameter was obtained after the acid treatment.

3.2. Thermal stability

The thermal stability of both CB and CBN was characterized using thermogravimetric analysis. In these experiments, the loss weight of the material was plotted as a function of temperature under air flow upon heating at 20 °C min^{-1} (Fig. 6). The TG curves show an initial drop between 50 and 150 °C which corresponds to a mass loss of absorbed moisture of approximately 12%. The initial decomposition temperature was 280 and 220 °C for CB and CBN, respectively, and it can be attributed to starch and cellulose depolymerization in both cases. In this step, the decomposition of CBN occurs at lower temperature than for CB. According to Roman and Winter (2004), the sulfuric acid hydrolysis was found to decrease the thermostability of bacterial cellulose crystals in agreement with our results.

Table 2
Main probable components of the CBN suspension determined by HPLC.

Retention time (min)	Codification	Probable component
6.37	a	Maltose
7.08	b	Maltose, cellobiose, sucrose
8.25	c	Glucose, sucrose
8.63	d	Sucrose
9.30	e	Fructose, xylose
10.20	f	Arabinose
10.75	g	n.i.(*)
12.32	h	n.i.(*)
13.40	i	Formic acid
14.58	j	Acetic acid
2.77	k	n.i.(*)

(*)n.i., not identified.

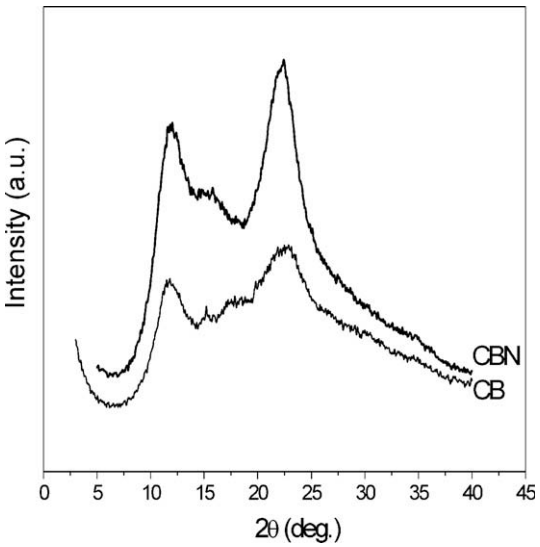

Fig. 5. X-ray diffraction patterns for CB and dried CBN.

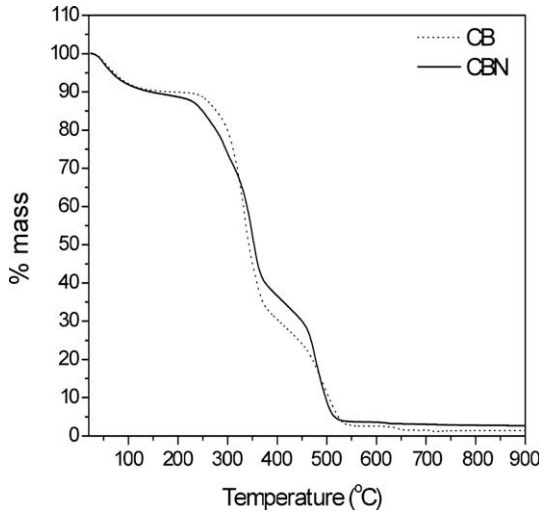

Fig. 6. TGA curves measured under air at 20 °C min^{-1} flow for CB and CBN.

3.3. Morphological investigation of nanocomposites

Fig. 7 shows the SEM observation of the fractured surface of the unfilled matrix plasticized with glycerol (panel A) or with the mixture of glycerol and sorbitol (panel C), and related nanocomposites reinforced with 20 wt% of CBN (panels B and D), respectively. The matrices display a relatively smooth surface as shown in Fig. 7A and C, while for nanocomposites the surface is rougher and more structured. The cellulosic nanoparticles appear as white dots in Fig. 7B and D and seem to be uniformly distributed.

3.4. Crystallinity and water uptake of nanocomposites

The X-ray diffraction patterns of nanocomposite samples after conditioning (10 days, 53% RH, 25 ± 2 °C) are shown in Fig. 8. Panels A and B correspond to materials plasticized with glycerol and with the mixture of glycerol/sorbitol, respectively. The diffraction pattern obtained for CBN has been added as reference. The different diffraction peaks are labeled in Fig. 8. The nanocomposite samples display a diffraction peak around $2\theta = 16.8°$ characteristic of amylopectin recrystallization (B-type crystallization). The processing-induced crystallization occurs as recrystallization of single-helical structure of amylose during cooling after processing. It corresponds to V_H-type and it is mainly characterized by the intense peak at $2\theta = 19.6^o$. The V_H-type consists of amylose recrystallization induced by lysophospholipids and complex-forming agents such as isopropanol and glycerol. The diffraction peaks corresponding to cellulose (CBN) at $2\theta = 12.5^o$ and $2\theta = 22.5°$ were not clearly observed in the diffraction patterns of nanocomposites.

No significant evolution of the peaks characteristics of the starch matrix was observed upon CBN addition, regardless the plasticizer. The crystallinity index was estimated from the magnitude of the diffraction peak located at $2\theta = 19.6°$ as reported in Section 2. Results are shown in Table 3. It is observed that the use of the glycerol/sorbitol mixture instead of pure glycerol results in a less crystalline material. This observation suggests that sorbitol should slightly hinder the complexation of glycerol with amylose. On the other hand, this behavior can be the consequence of the lower glycerol content present in TPSGS samples that decreases the amylose complexes resulting in a lower V_H-type crystalline structure. No changes were observed for the B-type crystallinity with respect to the nature of the plasticizer used.

However, it is worth noting that for nanocomposite samples filled with 20 wt% (for TPSG systems) and 10 and 20 wt% CBN (for TPSGS systems), a new diffraction peak located around $2\theta = 26.0^o$ (surrounded with broken line in Fig. 8) was observed. The magnitude of this peak increases with the CBN content for TPSGS samples. This peak was not present for the CBN sample and it is most probably related to the recrystallization of amylopectin in B-type structures (Van Soest, Hulleman, Wit, & Vliegenthar, 1996). Because this peak appears neither in the neat matrix nor in the poorly filled nanocomposites, it is most probably ascribed to an interfacial effect. This interfacial crystallization seems to be favored when the starch matrix is plasticized with the glyc-

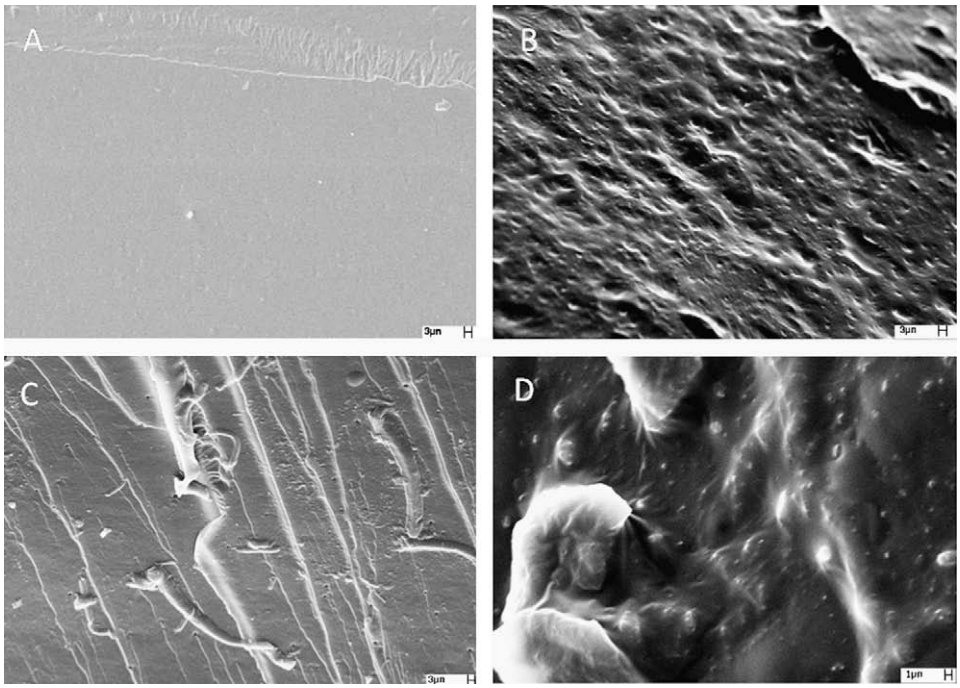

Fig. 7. Scanning electron micrograph of freshly fractured surface of TPSG (A), TPSG20 (B), TPSGS (C), and TPSGS20 (D).

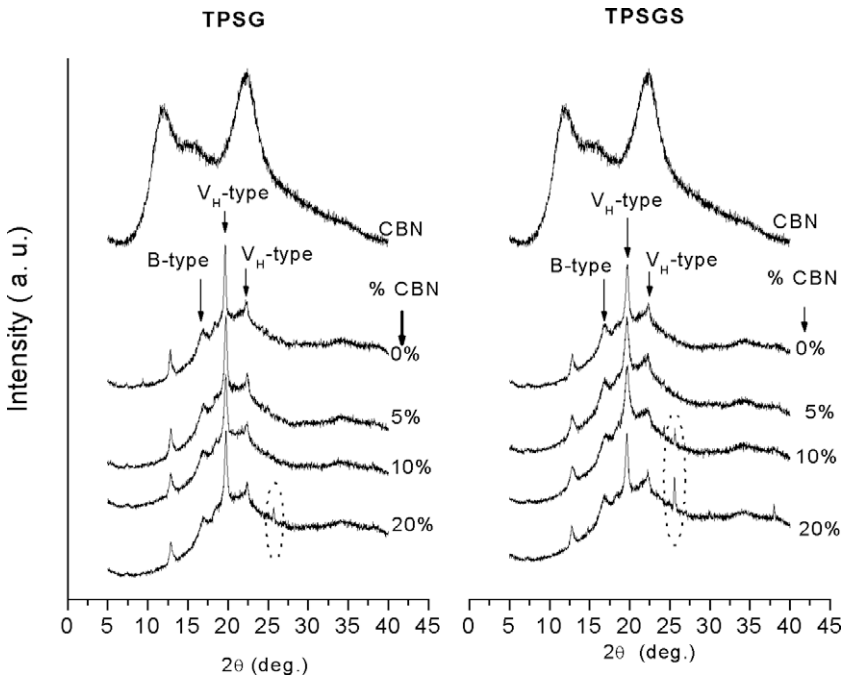

Fig. 8. X-ray diffraction patterns of conditioned samples (10 days, 25 °C, 53% RH): TPSG and related nanocomposites (A) and TPSGS and related nanocomposites (B).

Table 3
Quantitative characterization of crystallinity ($2\theta = 19.6°$) and water uptake at equilibrium (after 10 days conditioning at 25 ± 2 °C and 53% RH) for neat matrices and nanocomposites samples.

CBN content (wt%)	Crystallinity index ($2\theta = 19.6°$) (%)		Water uptake (%)	
	TPSG	TPSGS	TPSG	TPSGS
0	35	31	11.24 ± 0.11	9.30 ± 0.14
5	33	26	7.11 ± 0.10	7.65 ± 0.11
10	32	28	7.30 ± 0.08	7.70 ± 0.18
20	33	28	7.63 ± 0.06	7.90 ± 0.15

erol/sorbitol mixture. A transcrystallization phenomenon was reported for waxy maize starch plasticized with glycerol and reinforced with tunicin whiskers (Anglès & Dufresne, 2000, 2001) or starch nanocrystals (Angellier, Molina-Boisseau, Dole, & Dufresne, 2006).

The values of water uptake at equilibrium upon conditioning at room temperature and at 53% RH are collected in Table 3. The unfilled TPSG matrix is found to absorb more water than the unfilled TPSGS counterpart. It was reported that the water resistance of starch increased steadily with the molecular weight of the plasticizer and was directly proportional to the ratio of terminal to the total hydroxyl groups (Mathew & Dufresne, 2002). Adding CBN results in a decrease of the water uptake and the difference between the two matrices shades off. This means that the reduction of the hydrophilic nature due to CBN introduction was more effective for TPSG samples. The reduction of the water uptake is around 32–37% for TPSG and 15–18% for TPSGS. This phenomenon was ascribed to the formation of a cellulose nanoparticles network, which prevented the swelling of the starch and therefore its water absorption (Anglès & Dufresne, 2000).

3.5. Dynamic mechanical behavior

The evolution of the loss factor (tan δ) and logarithm of the storage tensile modulus (E', normalized at $E_{-100°C}$) as a function of temperature for TPSG and TPSGS samples is shown in Fig. 9A and B, respectively. Starch plasticized with either glycerol or glycerol/sorbitol behaves as a partially miscible system with two main relaxation phenomena evidenced through two maxima in tan δ curves. For TPSGS, the low temperature relaxation occurs around −30 °C and was attributed to the glass transition of the plasticizer (glycerol/sorbitol)-rich phase ($T_{g_{glycerol/sorbitol}}$). Pure sorbitol has a T_g around 0 °C and for pure glycerol the T_g value is around −75 °C (Mathew & Dufresne, 2002). Hence, a specific interaction between glycerol and sorbitol probably occurs owing to their chemical similarity. For TPSG samples, the relaxation phenomenon observed around −50 °C is associated with the T_g of glycerol-rich domains ($T_{g_{glycerol}}$).

For both systems, the high temperature relaxation corresponds to the glass transition of starch-rich domains ($T_{g_{starch}}$) and its temperature position is reported in Table 4 for both sets of nanocomposites. For the neat matrix, this relaxation phenomenon occurs at a lower temperature when using the glycerol/sorbitol mixture (25 °C) instead of glycerol alone (45 °C) as plasticizer. For TPSGS samples, the $T_{g_{starch}}$ value was not influenced by the CBN content, whereas it significantly decreased upon nanofibers addition for TPSG materials. No further evolution of $T_{g_{starch}}$ was reported upon increasing the CBN content and it was found to stabilize around 20 °C. A probable cause of the decrease of $T_{g_{starch}}$ for nanocomposites is the high sugar content present in the CBN suspension (mainly glucose and sucrose) and resulting from the hydrolysis of residual starch present in cassava bagasse. Teixeira, Da Róz, Carvalho, and Curvelo (2007) demonstrated that the addition of low

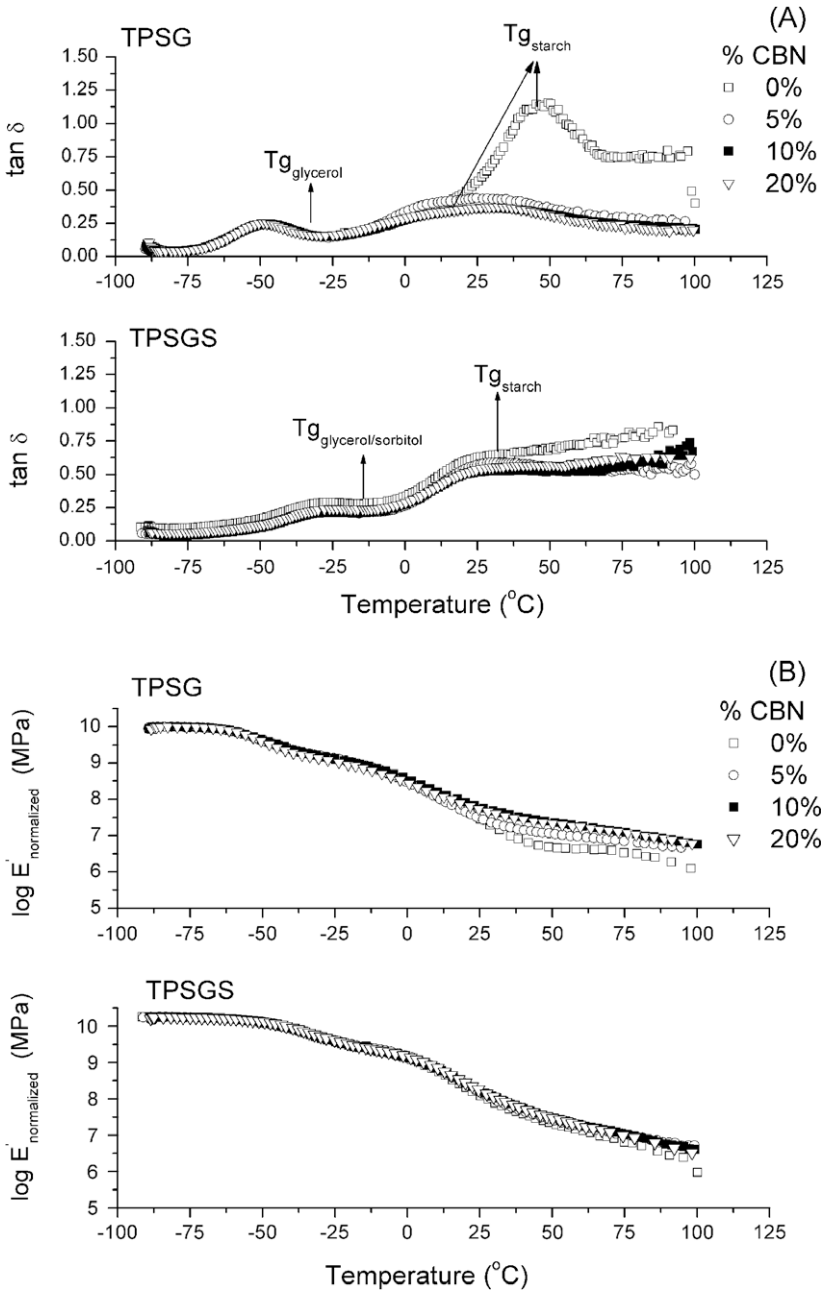

Fig. 9. Evolution of tan δ (A) and logarithm of storage modulus (B) as a function of temperature for TPSG and TPSGS samples reinforced with CBN after conditioning (10 days, 25 °C, 53% RH).

quantities of a sugar mixture (2 wt%, glucose, fructose, and sucrose, 1:1:1) to the starch–glycerol systems (30 wt% glycerol) causes a considerable reduction in $T_{g_{starch}}$ and inhibits the formation of V_H-type crystalline structures.

For TPSGS nanocomposites, this additional plasticizing effect induced by sugars originating from starch hydrolysis is not observed. The chemical similarity between starch and sugar, such as glucose, could favor interactions between starch and sugar components, reducing the specific interactions between the TPSG matrix and the nanofibers. Consequently, the mobility of starch chains is quite higher. The higher molecular weight of sorbitol as well as the higher OH content (182 g mol^{-1}) compared to glycerol (92 g mol^{-1}) restricts the chain mobility and the resulting materials are stiffer. These features are confirmed by the values of the storage modulus (see Fig. 9B and Table 4). The modulus value estimated at 25 °C for TPSGS materials is higher than for TPSG nanocomposites. However, because of the lower stiffness of the neat matrix, the relative reinforcing effect of CBN within the TPSG is more significant, mainly in the rubbery region (above 35 °C), than within the TPSGS matrix. It means that in the same temperature range, the effect of the filler

Table 4
Main relaxation temperature of the starch-rich phase ($T_{g_{starch}}$) determined from the maximum of tan δ peak and logarithm of the storage modulus (E') estimated at 25 °C, for the samples conditioned at 53% RH (10 days).

CBN content (wt%)	$T_{g_{starch}}$ (°C)		Log $E'_{(25°C)}$ (MPa)	
	TPSG	TPSGS	TPSG	TPSGS
0	45	25	7.40	8.06
5	20	25	7.45	8.15
10	20	25	7.72	8.22
20	20	25	7.72	8.24

for TPSGS materials is much lower. It is also worth noting that a transcrystallization phenomenon of the starch matrix was detected from X-ray diffraction experiments for TPSGS nanocomposites filled with 10 and 20 wt% cellulose nanofibers (Fig. 8), while for TPSG nanocomposites, such a phenomenon was observed only for 20 wt% cellulose nanofibers reinforced materials. This transcrystallization phenomenon obviously induces a decrease of cellulose nanofibers/starch interactions and consequently hinders the reinforcing effect of the nanofibers.

The evolution of the mechanical properties obtained from tensile tests, i.e., tensile strength; strain at break and tensile modulus, as a function of CBN content is shown in Fig. 10 for both TPSG and TPSGS systems. It is noted that for TPSG nanocomposites, the presence of sugar in CBN suspension probably cause a greater increase of elongation at break resulting in a weak reinforced effect. This increase of elongation suggests a major mobility for TPSG chains as verified by DMA analysis. For TPSGS systems this increase of elongation was not clearly observed. However, for 10% and 20% CBN reinforced TPSGS nanocomposites a significant decrease of the elastic modulus is observed. A possible transcrystallization phenomenon was reported from X-ray diffraction experiments (Fig. 8) for these compositions. This transcrystallization feature can induce a decrease of nanofibrils/starch interactions and consequently hinder the reinforcing effect of the filler. For TPSG, the transcrystallization was observed only for 20% of CBN (Fig. 8) and in this condition the increase of elastic modulus is inhibit.

4. Conclusions

This work shows that high added-value products can be obtained from an agricultural waste residue. All-cassava nanocomposite materials were processed. Cellulose nanofibrils with high length (360–1700 nm) and low diameter (2–11 nm) were directly extracted from cassava bagasse. The effect of these nanoparticles within a thermoplastic cassava starch matrix plasticized with glycerol or a mixture of glycerol and sorbitol was investigated. The presence of residual sugars and the nature of the plasticizer influence the final performance of the material. The glycerol/sorbitol mixture hinders the stress transfer at the filler/matrix interface probably because of the transcrystallization phenomenon of starch chains around the nanofibrils surface. It was clearly verified in r-x diffractogram profiles and the final modulus elastic. These phenomena seem to be more favored when using the glycerol/sorbitol mixture than when using glycerol alone. The reinforcing effect of these nanofibrils in glycerol plasticized starch was limited, especially because of an additional plasticization phenomenon induced by sugars originating from starch hydrolysis during the acid extraction. But, the CBN reinforced to cassava starch thermoplastic could be verified for all compositions.

The addition of cellulose nanofibers in the thermoplastic starch matrix results in a decrease of its hydrophilic character and capacity of water uptake especially for glycerol plasticized samples. As a future work, the isolation and bleaching of cellulose fibers from

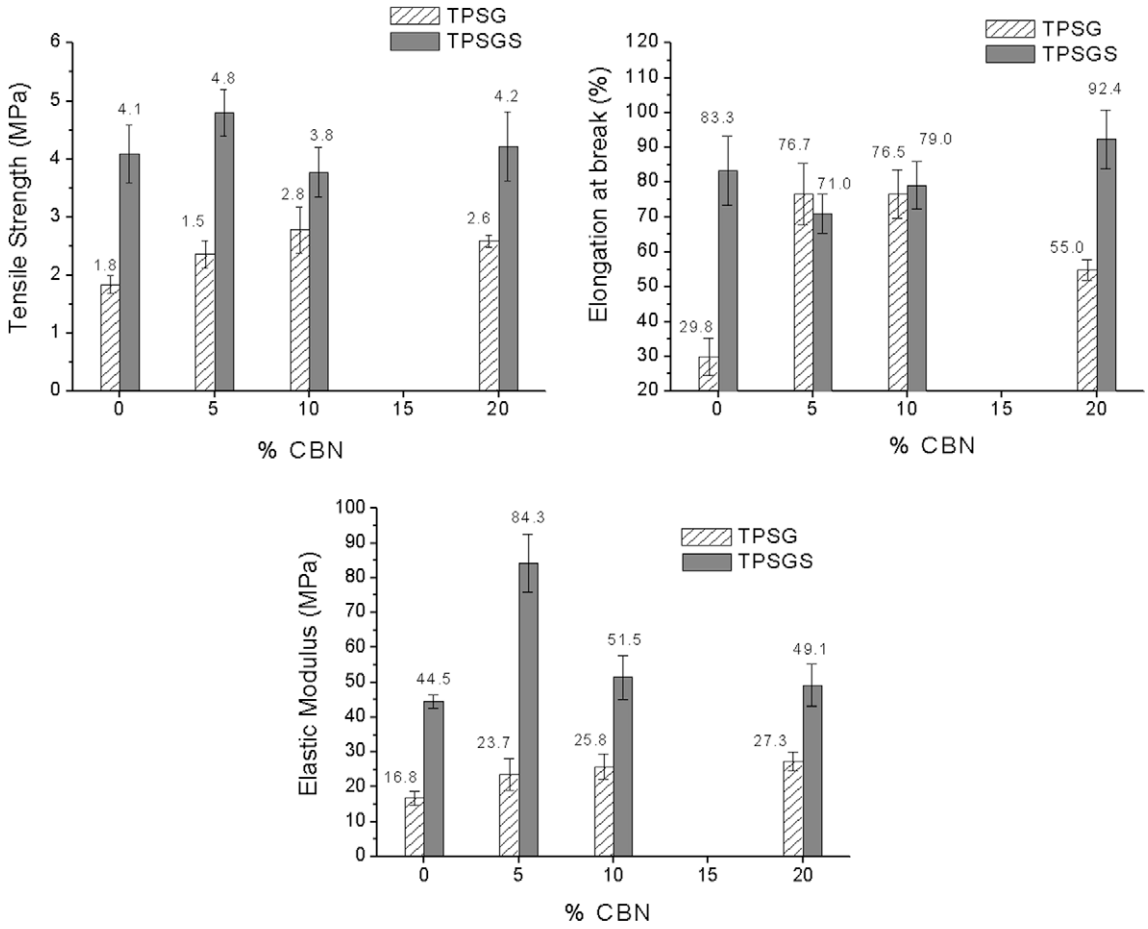

Fig. 10. Mechanical tensile properties of starch/CBN nanocomposites.

cassava bagasse before whiskers and/or nanofibers extraction is suggested. The effect of the resulting material as a reinforcing phase in a thermoplastic starch matrix is worth to be investigated.

Acknowledgments

The authors thank FAPESP (No. 03/13287-4), CAPES-COFECUB, and CNPq for financial support and Corn Products Brazil for supplying cassava starch samples.

References

Alemdar, A., & Sain, M. (2008). Isolation and characterization of nanofibers from agricultural residues – Wheat straw and soy hulls. *Bioresource Technology, 99*, 1664–1671.

Angellier, H., Molina-Boisseau, S., Dole, P., & Dufresne, A. (2006). Thermoplastic starch–waxy maize starch nanocrystals nanocomposites. *Biomacromolecules, 7*, 531–539.

Anglès, M. N., & Dufresne, A. (2000). Plasticized starch/tunicin whiskers nanocomposites. 1. Structural analysis. *Macromolecules, 33*, 8344–8353.

Anglès, M. N., & Dufresne, A. (2001). Plasticized starch/tunicin whiskers nanocomposites materials. 2. Mechanical behavior. *Macromolecules, 34*, 2921–2931.

Averous, L. (2004). Biodegradable multiphase systems based on plasticized starch: A review. *Journal of Macromolecular Science – Polymer Reviews, C44*, 231–274.

Azizi Samir, M. A. S., Alloin, F., & Dufresne, A. (2005). Review of recent research into cellulosic whiskers, their properties and their application in nanocomposite field source. *Biomacromolecules, 6*, 612–626.

Cherian, B. M., Pothan, L. A., Nguyen-Chung, T., Mennig, G., Kottaisamy, M., & Thomas, S. (2008). A novel method for the synthesis of cellulose nanofibril whiskers from banana fibers and characterization. *Journal of Agricultural and Food Chemistry, 56*, 5617–5627.

Curvelo, A. A. S., de Carvalho, A. J. F., & Agnelli, J. A. M. (2001). Thermoplastic starch–cellulosic fibers composites: Preliminary results. *Carbohydrate Polymers, 45*, 183–188.

Dufresne, A. (2006). Comparing the mechanical properties of high performances polymer nanocomposites from biological sources. *Journal of Nanoscience and Nanotechnology, 6*, 322–330.

Dufresne, A. (2008). Polysaccharide nano crystal reinforced nanocomposites. *Canadian Journal of Chemistry – Revue Canadienne de Chimie, 86*, 484–494.

Dufresne, A., Dupeyre, D., & Vignon, M. R. (2000). Cellulose microfibrils from potato tuber cells: Processing and characterization of starch–cellulose microfibril composites. *Journal of Applied Polymer Science, 76*, 2080–2092.

Gardner, D. J., Oporto, G. S., Mills, R., & Samir, M. A. S. A. (2008). Adhesion and surface issues in cellulose and nanocellulose. *Journal of Adhesion Science and Technology, 22*, 545–567.

Hulleman, S. H. D., Kalisvaart, M. G., Janssen, F. H. P., Feil, H., & Vliegenthart, J. F. G. (1999). Origins of B-type crystallinity in glycerol-plasticizer, compression-moulded potato starches. *Carbohydrate Polymers, 39*, 351–360.

John, R. P., Gangadharan, D., & Nampoothiri, K. M. (2008). Genome shuffling of *Lactobacillus delbrueckii* mutant and *Bacillus amyloliquefaciens* through protoplasmic fusion for L-lactic acid production from starchy wastes. *Bioresource Technology, 99*, 8008–8015.

John, R. P., Sukumaran, R. K., Nampoothiri, K. M., & Pandey, A. (2007). Statistical optimization of simultaneous saccharification and L(+)-lactic acid fermentation from cassava bagasse using mixed culture of lactobacilli by response surface methodology. *Biochemical Engineering Journal, 36*, 262–267.

Klemm, D., Heublein, B., Fink, H. P., & Bohn, A. (2005). Cellulose: Fascinating biopolymer and sustainable raw material. *Angewandte Chemie – International Edition, 44*, 3358–3393.

Kvien, I., Sugiyama, J., Votrubec, M., & Oksman, K. (2007). Characterization of starch based nanocomposites. *Journal of Materials Science, 42*, 8163–8171.

Kvien, I., Tanem, B. S, & Oksman, K. (2005). Characterization of cellulose whiskers and their nanocomposites by atomic force and electron microscopy. *Biomacromolecules, 6*, 3160–3165.

Lima, M. M. D., & Borsali, R. (2004). Rodlike cellulose microcrystals: Structure, properties, and applications. *Macromolecular Rapid Communications, 25*, 771–787.

Martin, C., Lopez, Y., Plasencia, Y., & Hernández, E. (2006). Characterisation of agricultural and agro-industrial residues as raw materials for ethanol production. *Chemical and Biochemical Engineering Quarterly, 20*, 443–447.

Martin, C., & Thomsen, A. B. (2007). Wet oxidation as a pretreatment of lignocellulosic residues of sugarcane, rice, cassava and peanuts for ethanol production. *Journal of Chemical Technology and Biotechnology, 82*, 174–181.

Mathew, A. P., & Dufresne, A. (2002). Morphological investigations of nanocomposites from sorbitol elasticized starch and tunicin whiskers. *Biomacromolecules, 3*, 609–617.

Matsui, K. N., Larotonda, F. D. S., Paes, S. S., Luiz, D. B., Pires, A. T. N., & Laurindo, J. B. (2004). Cassava bagasse-Kraft paper composites: Analysis of influence of impregnation with starch acetate on tensile strength and water absorption properties. *Carbohydrate Polymers, 55*, 237–243.

Nabeshima, E. H., & Grossmann, M. V. E. (2001). Functional properties of pregelatinized and cross-linked cassava starch obtained by extrusion with sodium trimetaphosphate. *Carbohydrate Polymers, 45*, 347–353.

Ngah, W. S. W., & Hanafiah, M. A. K. M. S. (2008). Removal of heavy metal ions from wastewater by chemically modified plant wastes as adsorbents: A review. *Bioresource Technology, 99*, 3935–3948.

Pääkko, M., Ankerfors, M., Kosonen, H., Nykänen, A., Ahola, S., Österberg, M., et al. (2007). Enzymatic hydrolysis combined with mechanical shearing and high-pressure. *Biomacromolecules, 8*, 1934–1941.

Pu, Y. Q., Zhang, J. G., Elder, T., Deng, Y., Gatenholm, P., Ragauskas, A., et al. (2007). Investigation into nanocellulosics versus acacia reinforced acrylic films. *Composites Part B – Engineering, 38*, 360–366.

Ray, R. C., Mohapatra, S., Panda, S., & Kar, S. (2008). Solid substrate fermentation of cassava fibrous residue for production of alpha-amylase, lactic acid and ethanol. *Journal of Environmental Biology, 29*, 111–115.

Roman, M., & Winter, W. T. (2004). Effect of sulfate groups from sulfuric acid hydrolysis on the thermal degradation behavior of bacterial cellulose. *Biomacromolecules, 5*, 1671–1677.

Teixeira, E. M., Da Róz, A. L., Carvalho, A. J. F., & Curvelo, A. A. S. (2007). The effect of glycerol/sugar/water and sugar/water mixtures on the plasticization of thermoplastic cassava starch. *Carbohydrate Polymers, 69*, 619–624.

Teixeira, E. M., Da Róz, A. L., de Carvalho, A. J. F., & Curvelo, A. A. S. (2005). Preparation and characterisation of thermoplastic starches from cassava starch, cassava root and cassava bagasse. *Macromolecular Symposia, 229*, 266–275.

Van Soest, J. J. G., Hulleman, S. H. D., Wit, D., & Vliegenthar, J. F. G. (1996). Crystallinity in starch bioplastics. *Industrial Crops and Products, 5*, 11–22.

Wollerdorfer, M., & Bader, H. (1998). Influence of natural fibers on the mechanical properties of biodegradable polymers. *Industrial Crops and Products, 8*, 105–112.

Zhang, J. G., Elder, T. J., Pu, Y. Q., & Ragauska, A. J. (2007). Facile synthesis of spherical cellulose nanoparticles. *Carbohydrate Polymers, 69*, 607–611.

Zhang, J., Jiang, N., Dang, Z., Elder, T. J., & Ragauska, A. J. (2008). Oxidation and sulfonation of cellulosics. *Cellulose, 15*, 489–496.

Zuluaga, R., Putaux, J. L., Cruz, J., Vélez, J., Mondragon, I., & Cañán, P. (2009). Cellulose microfibrils from banana rachis: Effect of alkaline treatments on structural and morphological features. *Carbohydrate Polymers, 76*, 51–59.

Zuluaga, R., Putaux, J. L., Restrepo, A., Mondragon, I., & Gañán, P. (2007). Cellulose microfibrils from banana farming residues: Isolation and characterization. *Cellulose, 14*, 585–592.